American Journal of Engineering Research (AJER)
e-ISSN: 2320-0847 p-ISSN : 2320-0936
Volume-14, Issue-2, pp-149-157
www.ajer.org
Research Paper Open Access

Research on the Preparation of Conductive Foam Materials and Their Piezo-resistive Properties

Hehe Zhou[1,*], Jie Lv[1], Haofeng Luo [1], Qiancheng Shu[1], Caowei Lu[1], Haofeng Shi[1], Jianfeng Qiu[1], Junqiang Lu[1], Qifeng Liang[1]and Chulei Zhong[1]
[1] *School of Mathematics Information, Shaoxing University, Shaoxing 312000,China;*

Abstract: *Conductive foam materials have attracted considerable attention due to their lightweight, porous structure, and conductive properties. This study focuses on polyurethane foam (PUF), in which sodium alginate (SA) is added during preparation. Conductive polyurethane composites are fabricated using physically doped conductive carbon black modified with sodium dodecylbenzenesulfonate and liquid styrene-butadiene rubber, and the material properties are subsequently explored.Experiments demonstrate that the SA content significantly affects the performance of PUF. At a concentration of 15%, the internal pore structure of PUF is uniform, exhibiting good flexibility, certain strength, and excellent mechanical stability. The prepared conductive polyurethane composite foam shows stable piezoresistive performance after 100 cycles of compression at a strain of 40%, exhibiting outstanding sensing characteristics. This study provides a theoretical and practical foundation for the application of conductive foam materials in electronic devices, sensors, and other fields, contributing to their widespread and precise utilization in more areas.*
Keywords: *conductive foam; polyurethane; sodium alginate; piezoresistive.*

Date of Submission: 20-02-2025 Date of acceptance: 03-03-2025

I. INTRODUCTION

In today's rapidly advancing technological era, the field of materials science is continuously introducing a variety of new materials with unique properties to meet the growing demands of different engineering and application scenarios. Among these, conductive foam materials, which combine lightweight, porous structures with conductive properties, are receiving increasing attention and research interest[1, 2].

Among the choices for conductive foam materials, polyurethane foam (PUF) is the most widely used. PUF has numerous advantages, including lightweight, high specific surface area, and good flexibility, due to its internal structure of interconnected pores. This makes it widely applicable in various traditional fields such as packaging, sound insulation, heat insulation, and adsorption filtration[3].When conductive properties are imparted to PUF, its application range is greatly expanded, enabling it to play a key role in cutting-edge fields such as electronic devices, sensors, electromagnetic shielding, and biomedicine[4-6]. Meanwhile, the piezoresistive properties of conductive PUF have become one of its most notable features in various applications. Piezoresistive properties refer to the phenomenon where the resistance of a material changes in response to external pressure.This property enables conductive PUF to serve as a promising material for pressure sensors, capable of real-time detection of the magnitude, distribution, and variations of external pressure[7].In practical applications, such as in wearable electronic devices, the piezoresistive properties of conductive PUF can be used to create flexible sensors capable of accurately monitoring human motion posture and physiological signals (such as pulse and joint activity)[8, 9]. In the field of smart insoles, it can detect the distribution of pressure on the soles of the feet during walking, providing important data for foot health monitoring and motion analysis[10, 11].

The preparation methods for conductive PUF are diverse, encompassing various techniques such as physical doping [12], chemical coating [13], and in situ polymerization [14].For example, by physically doping conductive fillers (such as carbon nanotubes, graphene, or metal powders) into the foam matrix, a conductive network is formed between the fillers, enabling the foam to acquire conductivity [15]. The chemical coating method, on the other hand, involves depositing a metallic conductive layer on the surface of the foam through chemical reactions, thereby imparting conductive properties [16].Different preparation methods can significantly affect the final microstructure, electrical conductivity, and other related physicochemical properties

of conductive foam materials. Therefore, selecting the appropriate fabrication process is crucial for obtaining desirable conductive foam materials.

In recent years, numerous studies have focused on using flexible PUF as the substrate for the fabrication of piezoresistive sensors [17].Cao et al. [18] soaked PUF in a graphene oxide (GO) solution for in situ chemical reduction, resulting in the fabrication of rGO/PUF composite sponges. The flexible piezoresistive sensors obtained exhibited good sensing performance, with a stress range of 0-3.2 kPa.Yao et al. [19] used graphene (GE) nanosheets as a conductive coating on PUF and combined it with a fractured microstructure design to fabricate large-area GE-coated PUF-based sensors. These sensors exhibited a sensitivity of 0.26 kPa^{-1} within a range of 0-2 kPa.However, the mechanical properties of the PUF substrates used in most flexible sensors currently have certain limitations, resulting in a relatively small pressure detection range that is not suitable for large-scale monitoring [20]. Additionally, there are still many unresolved issues regarding the optimization of their preparation processes and the in-depth understanding and precise control of their piezoresistive properties.For example, it is essential to explore whether the detection range of piezoresistive sensors can be expanded to accommodate a broader range of applications. Additionally, it is critical to investigate ways to further enhance the flexibility and stability of the materials while ensuring good electrical conductivity.

Given the significant application value of conductive foam materials in various fields and the existing issues in current research, this study incorporates sodium alginate (SA) during the preparation of PUF to investigate the effects of varying SA concentrations on the mechanical properties of the foam.At the same time, sodium dodecylbenzenesulfonate (SDBS) modified conductive carbon black (MCBB) and liquid styrene-butadiene rubber (SBR) are used to prepare conductive polyurethane composites through a physical doping method. The study explores the waterproof performance, micro-morphology, and piezoresistive properties of the composite material.It is hoped that this research will provide a solid theoretical and practical foundation for the broader and more precise applications of conductive foam materials in the future.

II. EXPERIMENTAL SECTION

2.1. Experimental Materials

Conductive Carbon Black (CB): Industrial grade, Hefei Kejing Material Technology Co., Ltd.; Sodium Dodecylbenzene Sulfonate (SDBS): Analytical grade, Shanghai Macklin Biochemical Technology Co., Ltd.; Sodium Alginate (SA): Analytical grade, Shanghai Aladdin Biochemical Technology Co., Ltd.Liquid Styrene-Butadiene Rubber (L-SBR): L-SBR-841N, Shanghai Aladdin Biochemical Technology Co., Ltd.; Polyether Polyol (PEP): Analytical grade, Shanghai Macklin Biochemical Technology Co., Ltd.; Toluene Diisocyanate (TDI): Analytical grade, Shanghai Macklin Biochemical Technology Co., Ltd.

2.2. Experimental Procedures

2.2.1. Preparation of High Porosity Polyurethane Foam

First, weigh 40 grams of PEP and take the corresponding amount of SA in a proportion of 0% to 25% based on the mass of TDI. Add these two components sequentially into a beaker and stir quickly at room temperature to ensure thorough mixing, labeling this mixture as raw material A.Additionally, take 14 grams of TDI and place it in a beaker as raw material B for later use.Next, heat raw materials A and B in a water bath to 85°C, while maintaining stirring at 350 r/min for raw material A during the heating process.Allow it to cool naturally to room temperature, then slowly pour raw material B into raw material A, immediately stirring at high speed until the mixture begins to foam, and then stop stirring. Finally, let the mixture sit for 2 hours to allow it to fully polymerize and foam, resulting in a highly porous polyurethane/sodium alginate material (PUF/SA).The content of SA added is 0%, 5%, 10%, 15%, 20%, and 25%, and the resulting materials are respectively named PUF/SA-0%, PUF/SA-5%, PUF/SA-10%, PUF/SA-15%, PUF/SA-20%, and PUF/SA-25%.Cut the materials into small cubes measuring 15 × 15 × 15 mm for subsequent experiments.

2.2.2. Preparation of MCCB

First, mix 2 g of CBwith 2 g of SDBS and ball mill the mixture for 2 hours. Then, transfer the mixture to a beaker, add 200 mL of deionized water, and sonicate for 2 hours.Next, perform centrifugation and wash the precipitate three times with deionized water to obtain the solid residue. Finally, dry the precipitate in a vacuum oven at 70°C for 24 hours to obtain MCCB, which can be ground and set aside for later use.

2.2.3. Preparation of Conductive Polyurethane Composites

Weigh 0.4 g of MCCB and dissolve it in 20 mL of deionized water. Subject the mixture to ultrasonic treatment for 30 minutes to obtain a conductive carbon black suspension.Subsequently, add 2 g of SBR to the suspension and use a ball mill to grind at high speed for 2 hours to ensure thorough mixing, resulting in MCCB/SBR conductive slurry.Immerse the cut and shaped PUF/SA cubes in the conductive slurry, press and soak for 5

minutes, then remove and place them in a vacuum oven to dry. This yields the conductive polyurethane composite (PUF/SA/MCCB/SBR).

2.3. Testing and Characterization

2.3.1. Microstructural Characterization

The cross-section of the PUF/SA foam samples was observed using a Zeiss Sigma 300 scanning electron microscope (SEM) to examine the sectional morphology and the pore framework structure.

2.3.2. Characterization of Apparent Density and Porosity

Select the cut and shaped PUF/SA samples, with four parallel specimens for each group. Weigh their mass and calculate the apparent density using formula (1) to obtain the average value. The porosity is calculated using formula (2).

$$\rho = \frac{m}{v}, \tag{1}$$

$$\Psi = \left(1 - \frac{\rho}{\rho_0}\right) \times 100\%, \tag{2}$$

In the equations, Ψ represents the porosity; ρ is the density of the foam material; ρ_0 is the density of the corresponding foam matrix (for polyurethane, ρ_0 = 1200 kg/m³).

2.3.3. Compression Performance Testing

Compression performance tests were conducted on the cut and shaped PUF/SA cubic samples at room temperature using a universal testing machine (Model ZQ-990C). Fix the samples horizontally at the center of the universal testing machine's platform, set the compression rate to 15 mm/min, and the compression stroke to 7.5 mm. Each group of samples is tested for 5 cycles. Use the accompanying testing software to output the real-time data of the pressure (kPa) changes for the PUF/SA materials.

2.3.4. Characterization of Specific Surface Area

The specific surface area and pore size distribution of CB and MCCB were measured using a specific surface area and pore size analyzer (Model BSD-PS2) by measuring and plotting the nitrogen adsorption-desorption isotherms. The specific surface area was calculated and the particle size analyzed. The degassing temperature was set at 300°C for a duration of 12 hours.

2.3.5. Piezoresistive Performance Testing

The piezoresistive performance testing was conducted using a universal testing machine in conjunction with a precision resistance tester (Model RK-2516N). Fix the obtained PUF/SA/MCCB/SBR samples horizontally at the center of the universal testing machine's platform, ensuring that the upper and lower surfaces of the samples are connected to the resistance tester to form an electrical circuit. Set the compression rate of the universal testing machine to 6 mm/min and the compression stroke to 6 mm, performing 100 cycles of compression testing. Collect the data on resistance (R) changes over time during the 100 cycles.

III. RESULTS AND DISCUSSION

3.1. Morphological Characterization of Polyurethanes with Different SA Content

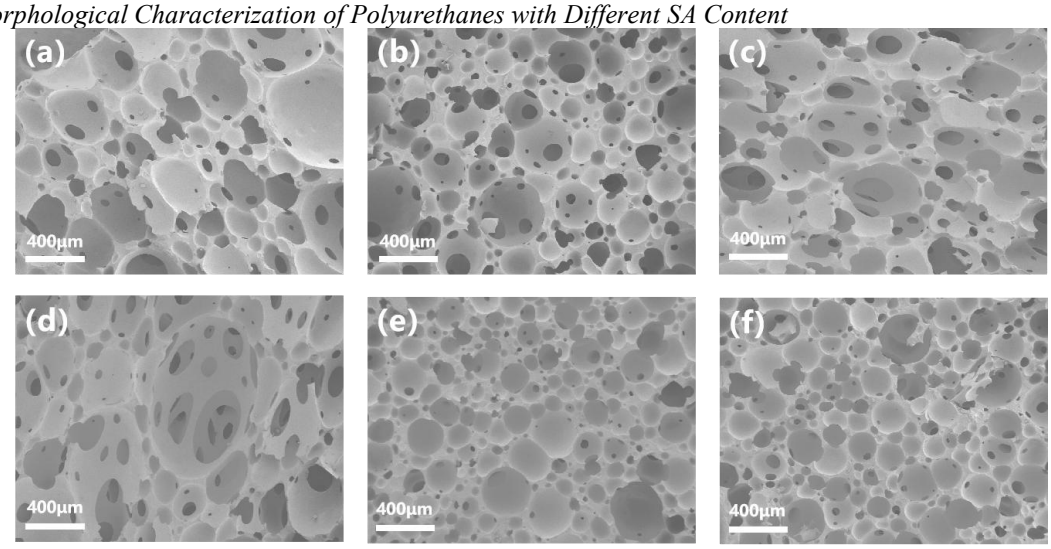

Figure 1. SEM images of the cross-section of PUF/SA composites: (a) PUF/SA-0%; (b) PUF/SA-5%; (c) PUF/SA-10%; (d) PUF/SA-15%; (e) PUF/SA-20%; (f) PUF/SA-25%.

Figure 1 shows the SEM images of the cross-section of PUF-SA composites with different amounts of SA added. Observing Figures 1a-d, it can be seen that when the SA content is 0, the pore size distribution is

uneven, and there is a tendency for hollow structures to form. With the increase in SA content, the internal pores of PUF-SA gradually become more uniform, forming a distinct three-dimensional network structure with well-defined interconnected pathways. However, when the SA content exceeds 20% (as shown in Figures 1e-f), the pore channel structure significantly decreases, accompanied by the phenomenon of foam wall accumulation. This indicates that when the SA content is 15%, the foam exhibits the optimal three-dimensional network structure, providing favorable conditions for subsequent compounding with conductive materials.

3.2. Characterization of Apparent Density and Porosity of PUF with Different SA Contents

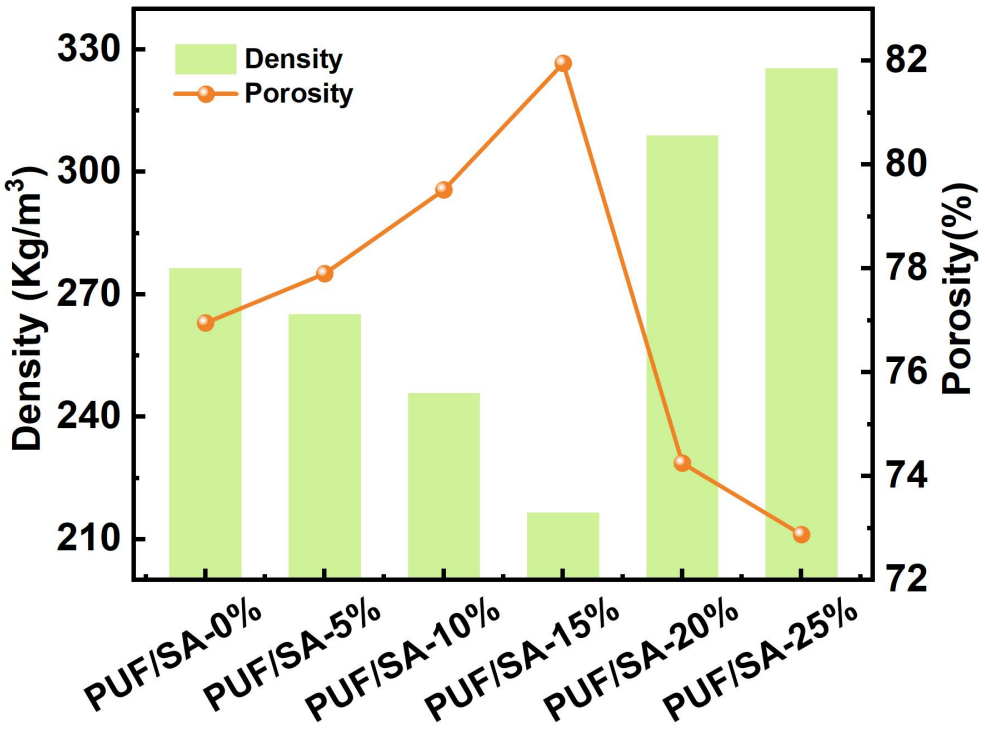

Figure 2. The Variation of Density and Porosity of PUF/SA.

Figure 2 shows the variation curves of density and porosity of PUF with different SA contents. It is evident from the figure that the introduction of SA has a significant impact on the density and porosity of PUF. With the increase in SA content, the density of PUF shows a trend of first decreasing and then increasing, while the porosity initially increases and then decreases. This change can be attributed to the imbalance between the foaming rate and the gelation rate when the SA content is below 15%. As the SA content gradually increases, the density of -NCO in the system decreases, which helps to balance the foaming rate and the gelation rate [21]. This balance facilitates the escape of CO2, resulting in the formation of more open pore structures. However, when the SA content exceeds 15%, the overall viscosity of the system increases, which hinders the escape of CO2. At the same time, the hydroxyl and carboxyl groups in SA, acting as polar groups, enhance the intermolecular interactions, leading to a decrease in the fluidity of the foaming mixture. This results in the accumulation of pore structures, which in turn increases the density of the foam [22]. This conclusion is consistent with the structural features observed in the cross-sectional SEM images of PUF/SA composites with different SA contents shown in Figure 1. Therefore, when the SA content is 15%, the porosity of PUF reaches its maximum value, demonstrating optimal flexibility.

3.3. Mechanical Performance Analysis

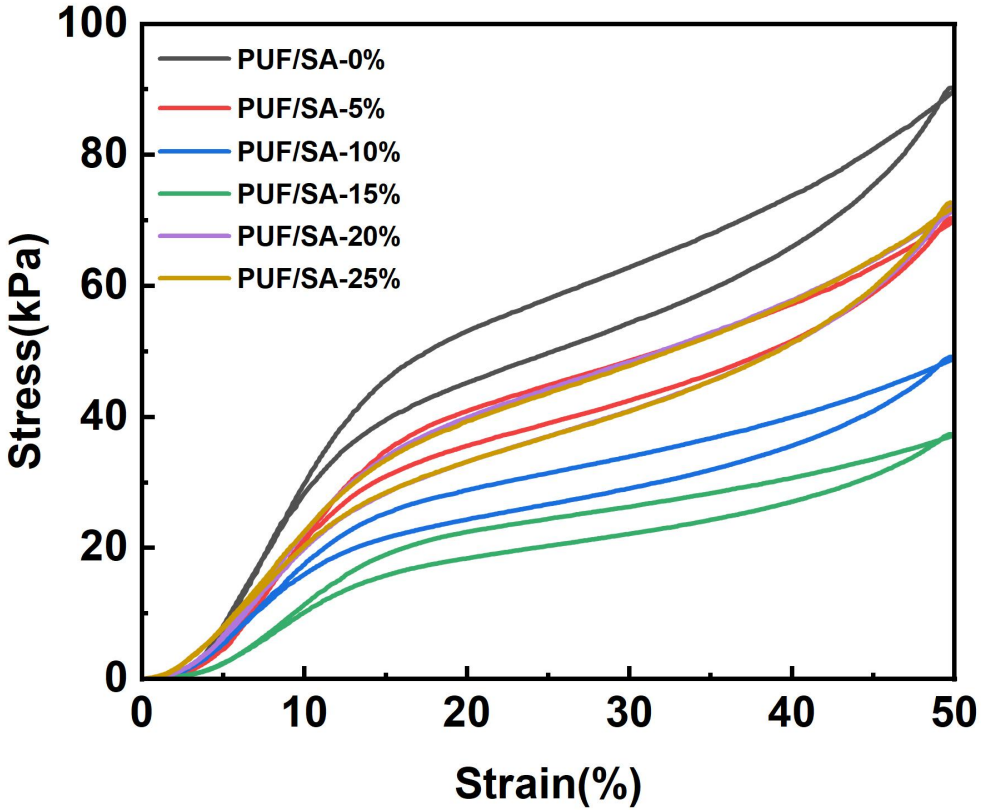

Figure 3. Compression Performance Graph of PUF/SA.

This study aims to explore and develop a PUF material that seeks to achieve an optimized balance between mechanical performance and flexibility while maintaining mechanical stability, thereby overcoming the limitations of traditional PUF materials, which struggle to attain both mechanical strength and flexibility. Figure 3 shows the compression recovery curves of PUF with different SA contents at 50% strain. The data from the figure indicate that as the SA content increases, the compressive hardness of the modified PUF/SA exhibits a trend of first decreasing and then increasing. Specifically, the compressive hardness of PUF/SA-0% is 90.18 kPa, which decreases to 70.27 kPa for PUF/SA-5%, further decreases to 49.16 kPa for PUF/SA-10%, and reaches the lowest value of 37.38 kPa for PUF/SA-15%. Subsequently, when the SA content increases to 20% and 25%, the compressive hardness rises to 72 kPa and 72.4 kPa, respectively. This trend is closely related to the microstructure of PUF. Observations from the SEM images reveal that when the SA content is between 0% and 15%, the through pores in PUF gradually increase, leading to an increased porosity and resulting in a softer foam. When the SA content exceeds 15%, the pores in the foam begin to close, resulting in a significant increase in compressive hardness [23]. Furthermore, for PUF as a flexible sensing material, a moderate reduction in compressive hardness contributes to enhancing the comfort on the skin.

Figure 4 illustrates the performance of PUF with different SA contents in compression cycle tests, aiming to investigate the effect of SA on the rebound performance of PUF.By observing Figures 4a-f, it can be seen that after five cycles of compression, although the load and unload curves of each foam do not fully overlap, the hysteresis loss loop shows a trend of gradually narrowing. Correspondingly, the hysteresis loss of the foam also decreases progressively [24].As the number of compression cycles further increases, the hysteresis loss of the foam tends to stabilize and no longer shows significant changes. This result strongly demonstrates that the foam material possesses good mechanical stability.Specifically, the hysteresis losses after five cycles of compression for Figures 4a-f are 9.55%, 7.1%, 8.39%, 9.67%, 8.82%, and 8.44%, respectively. These data indicate that the addition of a small amount of SA does not adversely affect the mechanical stability of the foam.By combining the previous analysis of the density and porosity variations of PUF with 0% to 25% SA content and the current compression cycle data, it can be concluded that when the SA content is at 15%, the prepared PUF not only exhibits moderate strength and flexibility but also possesses excellent mechanical stability.

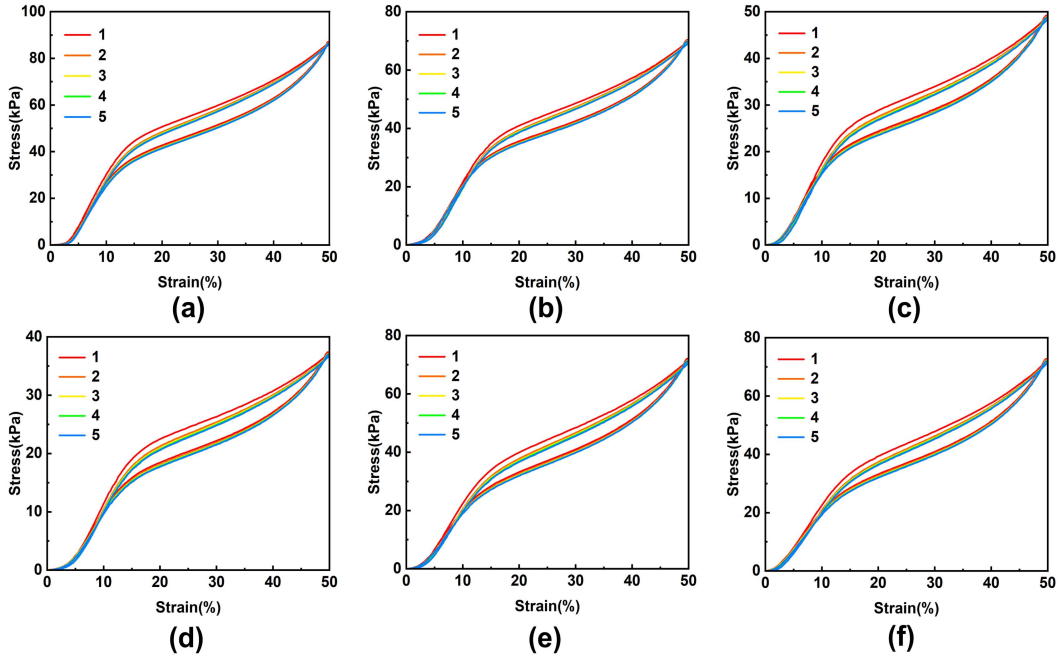

Figure 4. Compression Cycle Graph of PUF/SA: (a) PUF/SA-0%; (b) PUF/SA-5%; (c) PUF/SA-10%; (d) PUF/SA-15%; (e) PUF/SA-20%; (f) PUF/SA-25%.

3.4. Specific Surface Area of MCCB and Its Dispersion in Water.

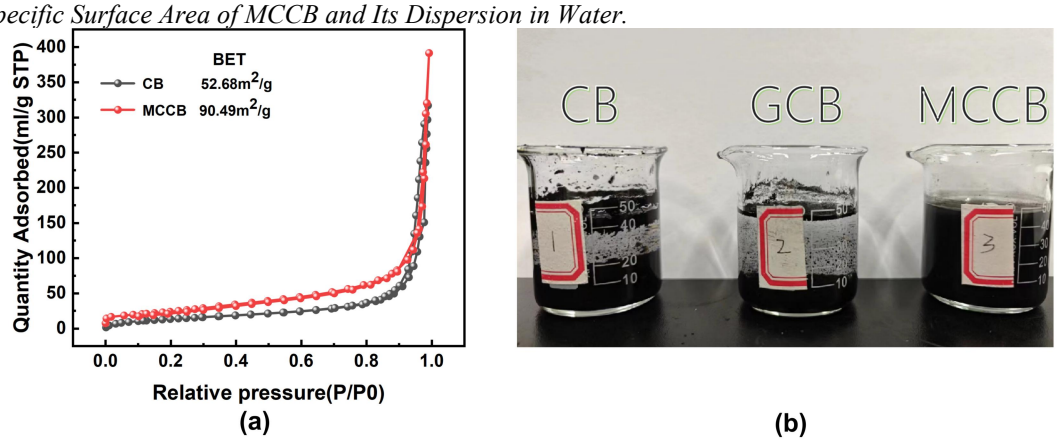

Figure 5. (a)Nitrogen adsorption−desorption isotherms of CB and MCCB;(b)Dispersibility in water of conductive carbon black.

As shown in Figure 5a, the specific surface areas of CB and MCCB materials were measured using nitrogen adsorption. The BET specific surface area of CB is 52.68 $m^2 g^{-1}$, while that of MCCB is significantly higher at 90.49 $m^2 g^{-1}$. This change indicates that the particle size of MCCB has notably decreased. Figure 5b shows the dispersion state of CB, ground carbon black (GCB), and MCCB after 30 minutes of ultrasonic treatment followed by a 2-hour standing period. It can be observed that MCCB exhibits good dispersion in water, forming a uniform and stable conductive carbon black suspension, with no sediment at the bottom of the beaker. In contrast, the beakers containing CB and GCB show floating particles on the liquid surface, and there is a noticeable sediment at the bottom of the beakers. This is due to the inherent tendency of CB to form highly aggregated and agglomerated structures, where strong van der Waals forces and other interactions between particles result in tight binding among them. When CB is placed in water, these aggregates are difficult to disperse by water molecules and instead settle or float as aggregates, exhibiting insoluble characteristics. However, after being activated and modified with SDBS, the surface of MCCB is coated with a layer of surfactant, which positions sodium ions on the outer layer, effectively improving the dispersion of conductive carbon black in water [25].

3.5. Piezoresistive Properties of PUF/SA/MCCB/SBR Composites.

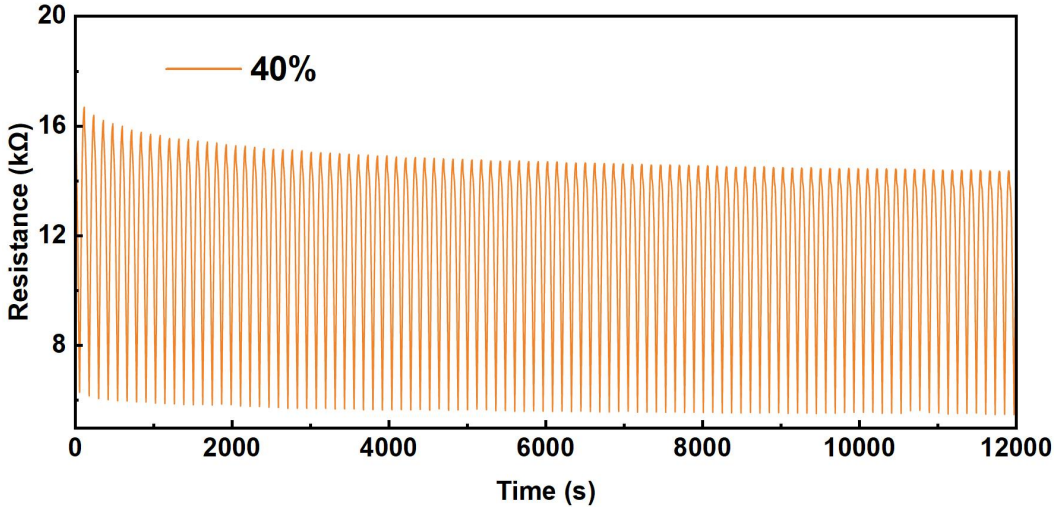

Figure 6. Resistance-Time (R-t) Curves of PUF/SA/MCCB/SBR Composites.

Stability is a key indicator of the durability and signal transmission stability of PUF as a piezoresistive sensor. In this study, PUF/SA was prepared with a selected SA content of 15%, and based on this, the piezoresistive properties of PUF/SA/MCCB/SBR were further developed and investigated. Figure 6 shows the R-t curves of PUF/SA/MCCB/SBR foam after 100 cycles of compression under a 40% strain condition. It can be clearly observed from the figure that throughout the 100 cycles of compression, the piezoresistive value of the foam gradually stabilizes between 6-15 kΩ, without significant fluctuations. This phenomenon clearly indicates that the prepared PUF/SA/MCCB/SBR foam exhibits good deformation adaptability in response to external pressure changes, thereby ensuring the stability of its piezoresistive properties and demonstrating its durability. This outstanding durability is primarily attributed to the incorporation of SBR, which allows the carbon black to adhere uniformly and firmly to the foam's framework, preventing any detachment even during repeated compression cycles, thereby ensuring the long-term stability of the piezoresistive properties of the composite foam.

IV. CONCLUSIONS

Through this in-depth study, it was found that when the addition of SA is controlled at 15%, the resulting PUF exhibits excellent overall performance. This foam not only possesses moderate strength and flexibility but also demonstrates outstanding mechanical stability. Additionally, through effective activation treatment with SDBS, MCCB exhibited excellent dispersion in water, successfully forming a uniform and stable conductive carbon black suspension. A PUF/SA/MCCB/SBR composite foam was designed and prepared, which maintained stable piezoresistive properties and a wide piezoresistive range (6-15 kΩ) even after undergoing 100 cycles of compression testing at 40% strain. This result strongly demonstrates that the composite foam exhibits good performance in sensing applications, providing robust material support for related fields.

Author Contributions: Conceptualization, J.Q.L., Q.F.L. and C.L.Z.; methodology, J.Q.L., Q.F.L. and C.L.Z.; investigation, H.H.Z., J.L., H.F.L., Q.C.S., H.F.S., J.F.Q.; resources, Q.F.L. and C.L.Z.; writing—original draft preparation, H.H.Z.; writing—review and editing, J.L., H.F.L., Q.C.S., H.F.S., J.F.Q, J.Q.L., Q.F.L. and C.L.Z.; visualization, H.H.Z. and J.L.; supervision, J.Q.L., Q.F.L. and C.L.Z.; project administration, J.Q.L., Q.F.L. and C.L.Z.. All authors have read and agreed to the published version of the manuscript.

Funding: This research received no external funding.

Institutional Review Board Statement: Not applicable.

Informed Consent Statement: Not applicable.

Data Availability Statement: The data that support the findings of this study are available upon reasonable request.

Conflicts of Interest: The authors declare no conflicts of interest.

REFERENCES

[1]. Tomin, M.; Lengyel, M. A.; Párizs, R. D.; Kmetty, A., Measuring and mathematical modeling of cushion curves for polymeric foams. Polymer Testing **2023,** 117.

[2]. Cho, D.; Park, J.; Kim, J.; Kim, T.; Kim, J.; Park, I.; Jeon, S., Three-Dimensional Continuous Conductive Nanostructure for Highly Sensitive and Stretchable Strain Sensor. ACS applied materials & interfaces **2017,** 9, (20), 17370-17379.

[3]. Dong, H. H.; Li, S. J.; Jia, Z. X.; Luo, Y. F.; Chen, Y. J.; Jiang, J.; Ji, S., A Review of Polyurethane Foams for Multi-Functional and High-Performance Applications. Polymers **2024,** 16, (22).
[4]. Su, Y.; Ma, K. A.; Mao, X. R.; Liu, M.; Zhang, X., Highly Compressible and Sensitive Flexible Piezoresistive Pressure Sensor Based on MWCNTs/Ti₃C₂T_x MXene @ Melamine Foam for Human Gesture Monitoring and Recognition. Nanomaterials **2022,** 12, (13).
[5]. Li, Z. X.; Gao, X. Y.; Huang, P.; Li, Y. Q.; Fu, S. Y., A flexible carbonized melamine foam/silicone/epoxy composite pressure sensor with temperature and voltage-adjusted piezoresistivity for ultrawide pressure detection. Journal of Materials Chemistry A **2022,** 10, (16), 9114-9120.
[6]. Wan, Y. B.; Wang, Y.; Guo, C. F., Recent progresses on flexible tactile sensors. Materials Today Physics **2017,** 1, 61-73.
[7]. Fiorillo, A. S.; Critello, C. D.; Pullano, S. A., Theory, technology and applications of piezoresistive sensors: A review. Sensors and Actuators A: Physical **2018,** 281, 156-175.
[8]. Han, S. T.; Peng, H. Y.; Sun, Q. J.; Venkatesh, S.; Chung, K. S.; Lau, S. C.; Zhou, Y.; Roy, V. A. L., An Overview of the Development of Flexible Sensors. Advanced materials **2017,** 29, (33).
[9]. Yuan, Y. Y.; Liu, B.; Li, H.; Li, M.; Song, Y. Q.; Wang, R. Z.; Wang, T. L.; Zhang, H. Y., Flexible Wearable Sensors in Medical Monitoring. Biosensors **2022,** 12, (12).
[10]. Li, W. D.; Zou, K. K.; Guo, J. W.; Zhang, C. C.; Feng, J. B.; You, J.; Cheng, G.; Zhou, Q. H.; Kong, M. Q.; Li, G. X.; Guo, C. F.; Yang, J. L., Integrated Fibrous Iontronic Pressure Sensors with High Sensitivity and Reliability for Human Plantar Pressure and Gait Analysis. ACS Nano **2024,** 18, (22), 14672-14684.
[11]. Zhang, P.; Wang, X. F.; Li, Y. X.; Zhang, K.; Huang, L. S., Plantar Pressure Monitoring System Based on a Flexible Pressure Sensor Array for Human Walking Feature Recognition. IEEE Transactions on Electron Devices **2023,** 70, (12), 6526-6533.
[12]. Nadafan, M.; Anvari, J. Z., Evaluation of structural, optical and physical properties of polyurethane composites doped with metal alkoxides. Materials Science-Poland **2020,** 38, (3), 416-423.
[13]. Loto, C. A., Electroless Nickel Plating - A Review. Silicon **2016,** 8, (2), 177-186.
[14]. Gong, X.; Liu, Q. T.; Chen, P. R.; Wang, H.; Liu, X. F.; Chen, S. C.; Wu, S. P., Modification mechanism of green polyurethane modified asphalt prepared by in-situ polymerization. Construction and Building Materials **2024,** 448.
[15]. Kim, Y.; Faseela, K. P.; Yang, S. Y.; Kim, K.; Yu, H. J.; Lim, J. Y.; Do, J. G.; Choi, H. R.; Hwang, J. H.; Baik, S., Excellent reversibility of resistive nanocomposite strain sensor composed of silver nanoflowers, polyurethane, and polyester rubber band. Composites Science and Technology **2022,** 221.
[16]. Tian, Q. H.; Guo, X. Y., Electroless copper plating on microcellular polyurethane foam. Transactions of Nonferrous Metals Society of China **2010,** 20, S283-S287.
[17]. Wang, Y. M.; Wang, X.; Li, X. L.; Bai, Y.; Xiao, H. H.; Liu, Y.; Liu, R.; Yuan, G. H., Engineering 3D Ion Transport Channels for Flexible MXene Films with Superior Capacitive Performance. Advanced Functional Materials **2019,** 29, (14).
[18]. Cao, W.; Luo, Y.; Dai, Y. M.; Wang, X.; Wu, K. L.; Lin, H. J.; Rui, K.; Zhu, J. X., Piezoresistive Pressure Sensor Based on a Conductive 3D Sponge Network for Motion Sensing and Human-Machine Interface. ACS Applied Materials & Interfaces **2023,** 15, (2), 3131-3140.
[19]. Liu, J.; Zhang, H. B.; Xie, X.; Yang, R.; Liu, Z. S.; Liu, Y. F.; Yu, Z. Z., Multifunctional, Superelastic, and Lightweight MXene/Polyimide Aerogels. Small **2018,** 14, (45).
[20]. Han, S.; Li, S.; Fu, X.; Han, S. H.; Chen, H. Y.; Zhang, L.; Wang, J.; Sun, G. H., Research Progress of Flexible Piezoresistive Sensors Based on Polymer Porous Materials. ACS Sensors **2024,** 9, (8), 3848-3863.
[21]. Burkhart, G.; Kollmeier, H.; Schloens, H., The importance of catalysts for the formation of flexible polyurethane foams. Journal of Cellular Plastics **1984,** 20, (1), 37-41.
[22]. Zhao, W.; Ma, L. Y.; Wang, Z. S.; Wang, F.; Zhang, L.; Ma, H. Z.; Wang, W., Preparation and characterization of highly stable double-crosslinked gel foam for inhibiting coal spontaneous combustion. Colloids and Surfaces A: Physicochemical and Engineering Aspects **2024,** 685.
[23]. Jiang, J.; Zhou, M.; Li, Y.; Chen, B.; Tian, F.; Zhai, W., Cell structure and hardness evolutions of TPU foamed sheets with high hardness via a temperature rising foaming process. The Journal of Supercritical Fluids **2022,** 188, 105654.
[24]. Hilyard, N. C., Hysteresis and energy loss in flexible polyurethane foams. Springer Netherlands **1994,** 226-229.
[25]. Nazari, B.; Ranjbar, Z.; Hashjin, R. R.; Moghaddam, A. R.; Momen, G.; Ranjbar, B., Dispersing graphene in aqueous media: Investigating the effect of different surfactants. Colloids and Surfaces A: Physicochemical and Engineering Aspects **2019,** 582.